HHS Public Access

Author manuscript

Acta Biomater. Author manuscript; available in PMC 2016 December 01.

Published in final edited form as:

Acta Biomater. 2015 December ; 28: 23–32. doi:10.1016/j.actbio.2015.09.018.

Combination Therapy of Stem Cell Derived Neural Progenitors and Drug Delivery of Anti-Inhibitory Molecules for Spinal Cord Injury

Thomas S. Wilems, **Jennifer Pardieck**, **Nisha Iyer**, and **Shelly E. Sakiyama-Elbert**

Department of Biomedical Engineering, Washington University, St. Louis, MO 63130

Abstract

Regeneration of lost synaptic connections following spinal cord injury (SCI) is limited by local ischemia, cell death, and an excitotoxic environment, which leads to the development of an inhibitory glial scar surrounding a cystic cavity. While a variety of single therapy interventions provide incremental improvements to functional recovery after SCI, they are limited; a multifactorial approach that combines several single therapies may provide a better chance of overcoming the multitude of obstacles to recovery. To this end, fibrin scaffolds were modified to provide sustained delivery of neurotrophic factors and anti-inhibitory molecules, as well as encapsulation of embryonic stem cell-derived progenitor motor neurons (pMNs). *In vitro* characterization of this combination scaffold confirmed that pMN viability was unaffected by culture alongside sustained delivery systems. When transplanted into a rat sub-acute SCI model, *fibrin scaffolds containing growth factors (GFs), anti-inhibitory molecules without pMNs, or pMNs with GFs had lower chondroitin sulfate proteoglycan levels compared to scaffolds containing anti-inhibitory molecules with pMNs*. Scaffolds containing pMNs, but not anti-inhibitory molecules, showed survival, differentiation into neuronal cell types, axonal extension in the transplant area, and the ability to integrate into host tissue. However, the combination of pMNs with sustained-delivery of anti-inhibitory molecules led to reduced cell survival and increased macrophage infiltration. While combination therapies retain potential for effective treatment of SCI, further work is needed to improve cell survival and to limit inflammation.

Graphical abstract

*To whom correspondence should be addressed: Shelly E. Sakiyama-Elbert, Department of Biomedical Engineering, 1097 Brookings Dr., Washington University in St. Louis, St. Louis, MO 63130, Ph: (314) 935-7556, Fax: (314) 935-7448, sakiyama@wustl.edu.

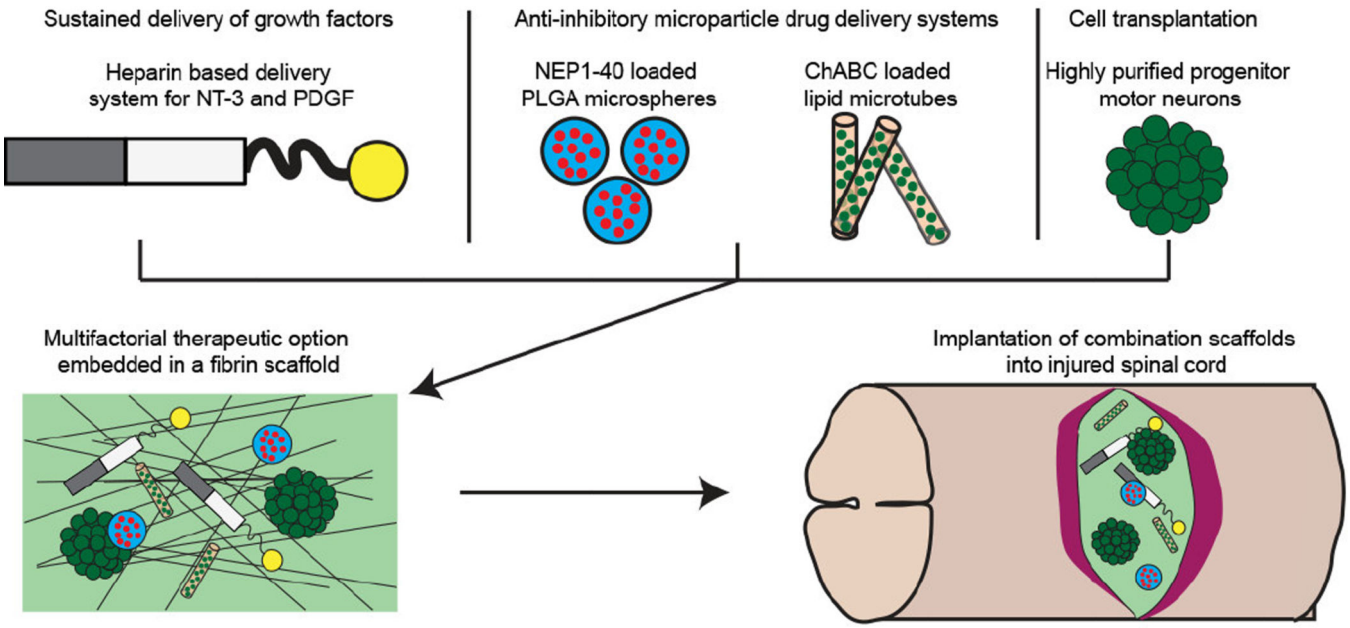

Keywords

PLGA microspheres; lipid microtubes; chondroitinase ABC; NEP1–40; controlled release; progenitor motor neurons

Introduction

Spinal cord injury (SCI) typically results from mechanical trauma that severs axons, damages vasculature, and promotes a secondary injury that results in cell death, leading to the formation of a cystic cavity and inhibitory glial scar, which act as chemical and physical barriers to regeneration. The variety of local and systemic changes caused by SCI creates a multitude of obstacles limiting recovery, which together hinder the effectiveness of single therapeutic interventions. This challenge has prompted the development of combination strategies that work together synergistically to improve recovery.

One major therapeutic strategy following SCI is cell transplantation. A wide variety of cell types have been investigated with emphasis placed on transplanting cells that are relevant to the central nervous system (CNS), such as neural progenitors, astrocytes, oligodendrocytes, and neurons [1–5]. Embryonic stem cells (ESCs) induced to form neural progenitor cells are promising, but have poor survival post-transplantation (~10% in the absence of scaffold); cells that do survive typically differentiate into glia with poor neuronal differentiation and maturation [6–10]. Furthermore, one significant drawback to the use of ESC-derived neural cells is the potential formation of teratomas due to the presence of undifferentiated ESCs in the transplant [11]. To address these concerns, differentiation protocols have been developed to obtain more restricted progenitor populations, including progenitor motor neurons (pMN), which give rise to motoneurons, oligdendrocytes and type II astrocytes [12, 13]. To further improve the purity of ESC-derived cells, our lab has developed a transgenic mouse ESC line

(P-Olig2) that expresses antibiotic resistance under the lineage-specific pMN marker, Olig2, which allows for positive selection of ESC-derived pMNs after induction [14].

Another therapeutic strategy is the delivery of pro-regenerative neurotrophic factors that are normally secreted by local glia and are vital to the maintenance of healthy tissue. Following injury, specific factors are upregulated within the spinal cord and help reduce cell death. Exogenous delivery of a variety of neurotrophic factors has been shown to increase cell survival and limit formation of the glial scar [15–23]. Delivery of platelet-derived growth factor (PDGF)-AA can aid the stabilization and maturation of blood vessels at the injury site and is an important factor in oligodendrocyte maturation [24–26], while neurotrophin 3 (NT-3) promotes regeneration of the corticospinal tract and dorsal sensory axons [15, 16]. When NT-3 and PDGF-AA were delivered from modified fibrin scaffolds capable of sustained release alongside ESC-derived pMNs, there was an increase in expression of neuronal markers both rostral and caudal to the injury site and improved migration of transplanted cells into the host spinal cord [14].

A third therapeutic approach is to limit the effects of the inhibitory environment surrounding the injury site using anti-inhibitory molecules. Two major inhibitory factors that are significantly upregulated after SCI are chondroitin sulfate proteoglycans (CSPGs) and myelin-associated inhibitors (MAIs), which form a biochemical barrier to axon growth [27, 28]. Under normal conditions, CSPGs are major components of perineuronal nets and are found within CNS extracellular matrix [29]. Inhibition by CSPGs is caused by the glycosaminoglycan (GAG) side chains, which are able to interact with target receptors on neuronal membranes [30–32]. Treatment with chondroitinase ABC (ChABC) cleaves the GAG side chains and prevents activation of target receptors [33–38].

MAIs, such as Nogo-A, oligodendrocyte-myelin glycoprotein, and myelin-associated glycoprotein, are important chemical cues in the mature CNS that limit axon growth and stabilize functional neuronal circuits [39, 40]. However, following SCI MAIs are not degraded or removed from the injury site, which results in limited axonal sprouting and regeneration [41]. Most MAIs interact with neurons through a common receptor, the Nogo receptors (NgR1 and NgR3), which initiate the Rho/ROCK cascade resulting in microtubule disassembly and growth cone collapse [42–45]. Although MAIs bind other receptors, inhibition of NgR1 using a small competitive antagonist (NEP1–40) significantly improved neurite outgrowth on myelin inhibitory substrates and improved functional recovery in rat SCI models [46]. Both types of anti-inhibitory molecules are typically delivered using invasive intrathecal pumps, catheters, or microinjections, which have the potential for increased scarring and compression of the spinal cord [47]. Drug delivery using anti-inhibitory microparticle systems (AIMS) within fibrin scaffolds are able to provide sustained local delivery of ChABC and/or NEP1–40 in a minimally invasive way. Using AIMS to deliver ChABC and NEP1–40, decreased CSPG deposition and increased axon sprouting were observed in a rat acute SCI model [48].

The combined delivery of cells, neurotrophic factors, and AIMS may lead to improved recovery compared to any single treatment alone. To this end, we incorporated ESC-derived pMNs and sustained drug delivery systems for anti-inhibitory molecules and neurotrophic

factors into fibrin scaffolds and tested their efficacy in both *in vitro* and *in vivo* models. To confirm their potential prior to transplantation, pMNs were cultured within biomaterial scaffolds containing the drug delivery systems for two weeks to measure cell viability *in vitro*. The combination scaffolds were then transplanted into a sub-acute rat SCI model to repopulate cells lost following injury, increase host and transplant cell survival, and reduce the local inhibitory environment. Transplantation of AIMS within fibrin scaffolds did not affect the presence of CSPGs within the glial scar compared to transplantation of pMNs with growth factors or growth factor delivery alone, but the presence of CSPGs increased when pMNs were combined with AIMS. While pMNs transplanted into fibrin scaffolds alone were viable and able to differentiate into neurons and astrocytes, a decrease in cell survival was observed when pMNs were transplanted in combination with AIMS, possibly due to elevated macrophage infiltration.

Materials and Methods

Embryonic Stem Cell Culture

A previously established transgenic ESC line (P-Olig2) was used for transplantation [49]. The P-Olig2 cell line contains the puromycin N-acetyltransferase (PAC) gene under the control of the native Olig2 regulatory elements in one allele, thus conferring puromycin resistance to cells expressing Olig2 after induction and allowing for positive selection of pMNs. To allow tracking of these cells, enhanced green fluorescent protein (GFP) was randomly inserted under the control of the β-actin promoter to provide ubiquitous reporter expression throughout the experiments [14, 49–51]. P-Olig2 ESCs were grown in complete media consisting of Dulbecco's modified Eagle's Medium (Life Technologies, Carlsbad, CA) supplemented with 10% newborn calf serum (Life Technologies), 10% fetal bovine serum (Life Technologies), and 1:200 100× EmbryoMax® Nucleosides (EMD Millipore, Billerica, MA). Cells were passaged at a 1:5 ratio every 2 days and seeded on a new T-25 flask coated with a 0.1% gelatin solution (Sigma). To avoid the use of a feeder cell layer, 1000 U/mL leukemia inhibitory factor (LIF; EMD Millipore) and 100 μM β-mercaptoethanol (BME; Life Technologies) were added to the media to maintain ESCs in an undifferentiated state [49, 52].

Progenitor Motor Neuron Induction

For pMN induction, P-Olig2 ES cells were exposed to retinoic acid (RA; Sigma) and smoothened agonist (SAG; EMD Millipore) in a $2^{-}/4^{+}$ induction protocol [49]. One million ESCs were aggregated into embryoid bodies (EBs) in 100-mm Petri dishes coated with a 0.1% agar solution in DFK5 media consisting of DMEM:F12 base media (Life Technologies) supplemented with 5% knockout serum replacement (Life Technologies), 50 μM non-essential amino acids Life Technologies),1:100 100× Insulin-Transferrin-Selenium (Life Technologies), 1:200 100× EmbryoMax® Nucleosides. EBs were allowed to form for 2 days in the absence of induction factors (2^{-}). EBs were then cultured in DFK5 supplemented with 2 μM RA and 0.5 μM SAG for the final four days (4^{+}). Media was changed every 2 days. In selected cultures, 4 μg/mL puromycin (Sigma) was added during the final 2 days of induction [49].

Formation of Poly(lactic-*co*-glycolic acid) (PLGA) Microspheres

PLGA microspheres, with a 50:50 lactic acid to glycolic acid ratio, were fabricated using a water in oil in water double emulsion solvent evaporation technique [53]. PLGA (10% w/v, intrinsic vis. = 0.15–0.3 dL/g, Absorbable Polymers Inc., Pelham, NJ) was dissolved in 2 mL dichloromethane (DCM). 100 μL of 10 mg/mL NEP1–40 (Mw = 4627 Da, Sigma) was added to the PLGA/DCM solution and sonicated for 10 seconds (Microson, Misonix Inc.), added to 25 mL of water with 1% w/v poly(vinyl alcohol) and 10% w/v NaCl and homogenized. The resulting emulsion was poured into 250 mL of water with 0.1% w/v poly(vinyl alcohol) and 10% w/v NaCl, then magnetically stirred for 3 hours, washed with water, frozen overnight at −80°C and lyophilized. PLGA microspheres were imaged using a scanning electron microscope (Nova NanoSEM 230, FEI) after gold sputter coating for 45 seconds. Diameters from individual microspheres were measured using ImageJ software and 100 microsphere diameters were averaged per batch.

Formation of Lipid Microtubes

Lipid microtubes were formed similar to previous work [54]. 1,2-bis(tricosa-10,12-diynoyl)-*sn*-3-phosphocholine ($DC_{8,9}PC$) lipids (Avanti Polar Lipids, Alabaster, AL) were dissolved at 55°C in 70% ethanol at 1 mg/mL and placed into a temperature controlled water bath (Haake A10, ThermoScientific, Asheville, NC). The total volume per batch was 5 mL. The temperature was decreased from 55°C to 25°C at a rate of 2.5°C/min. The lipid tubes were then stored at room temperature in the dark for one week. Trehalose (EMD Millipore) was added to a final concentration of 50 mM, the solution was centrifuged (1200 rcf, 5 minutes) to pellet the lipid microtubes, and 4 mL of solution was removed. The concentrated (5 mg/mL) microtube solution was lyophilized overnight to dry and stored at −20°C until further use. Prior to use 10 mg of dried microtubes were rehydrated with 100 μL of 500 mU/mL ChABC dissolved in 1 M trehalose for 2 hours at 4°C. After loading with ChABC, the solution was diluted with 15 mL of tris buffered saline (TBS), pH 7.4, then centrifuged (1200 rcf, 5 minutes) and the supernatant was removed. This step was performed one more time and the resulting loaded microtube pellet was used in 3D fibrin scaffold cultures or scaffold implantation into rat spinal cords.

3D Fibrin Scaffold Cultures

Fibrin scaffolds were prepared by dissolving fibrinogen (50 mg/mL; EMD Millipore) in TBS and dialyzing in 4L TBS for 24 hours. Fibrinogen was then sterile filtered before adjusting the concentration to 20 mg/mL as measured by UV spectroscopy. As previously described, a solution (150 μL) containing 10 mg/mL fibrinogen, 2.5 mM $CaCl_2$ (Sigma), and 2 NIH units/mL thrombin (Sigma) was mixed in a 48 well plate [52, 55]. For incorporation of AIMS, the fibrin scaffolds were mixed with 45 mg NEP1–40-loaded PLGA microspheres and 7.5 mg ChABC-loaded lipid microtubes. All scaffolds were washed 5 times with 500 μL TBS per wash over a 24 hour period to remove unbound delivery system components (heparin and/or growth factors).

Three to five EBs containing pMNs were placed on each fibrin scaffold, and an additional fibrin scaffold (100 μL) with only $CaCl_2$ and thrombin was added to the top of the EBs. The 48 well plates containing fibrin scaffolds with EBs were incubated for 1 hour at 37°C. Cell

media (500 μL) containing a 1:1 ratio of DFK5 media and Neurobasal (NB) (Life Technologies) media with 2% B27 supplement (Life Technologies) and 5 μg/mL aprotinin (Sigma) was then added to the top of the scaffolds. The EBs were cultured for 2 weeks with a single media change on day 3 to change to NB media with 2% B27 supplement and 5 μg/mL aprotinin.

Flow Cytometry

For evaluation of cell survival following 2 weeks of 3D culture, 0.25% trypsin-EDTA was added for 15 min to dissociate the EBs. pMNs from 2 scaffolds within the same group were combined together, triturated into a single cell suspension, then quenched with complete media. Cells were pelleted by centrifugation (5 min at 230×g), the supernatant was removed, and a standard LIVE/DEAD® Cell Viability Assay (Life Technologies) was performed. Live cells were identified by the incorporation of the membrane permeable calcein AM stain within a cell, whereas dead cells were identified by the binding of ethidium homodomer-1 to the nucleic acids of cells with damaged plasma membrane. Stained cells were analyzed for percent alive and dead using a Canto II flow cytometer (Becton Dickinson, Franklin Lakes, NJ). For each group, 30,000 events were recorded and FloJo software (FloJo, Ashland, OR) was used for population gating following debris removal based on forward scatter versus side scatter. Results from flow cytometry are reported as the percentage of cells staining positive for the live cellular marker or dead cellular marker out of the total cell population.

Spinal Cord Injury and Scaffold Implantation

Experiments performed on animals complied with the NIH Guide for the Care and Use of Laboratory Animals and were performed under the supervision of the Division of Comparative Medicine at Washington University. Prior to surgery, animals (female Long-Evans rats, 250–275 g) were anesthetized with 5% isoflurane gas and an injection of 5 mg/kg xylazine. An incision was made through the back to expose the back muscle. Parallel cuts were made through the muscle on each side of the vertebral processes from T6-T10. To expose the spinal cord, the dorsal lamina was removed at T8 with fine tip rongeurs. The spinal cord was stabilized using spinal clamps placed in the vertebral foramina at T7 and T9. Dura mater was removed and vitrectomy scissors attached to a micromanipulator were lowered 1.5 mm into the spinal cord. Using the vitrectomy scissors, a lateral dorsal hemisection was performed on the spinal cord. Following removal of the vitrectomy scissors and micromanipulator, the spinal cord was covered with artificial dura, the back muscles closed with degradable sutures, and the skin was stapled closed. Animals were given cefazolin (25 mg/kg) and buprenorphine (0.04 mg/kg) [50]. Cefazolin was continued twice daily for 5 days with buprenorphine (0.04 mg/kg) provided twice daily for 3 days and (0.01 mg/kg) for the next 3 days. Throughout the study, bladders were manually expressed twice a day until normal bladder function returned. Two weeks after the dorsal hemisection, the spinal cord was re-exposed, and a cavity for implantation was made by removing the scar tissue. Multifactorial fibrin scaffolds (300 μL) were prepared by mixing 10 mg/mL fibrinogen, 2.5 mM $CaCl_2$, 2 NIH units/mL thrombin, 62.5 μM heparin, 0.25 mM ATIII peptide, 125 ng NT3, 20 ng PDGF-AA, 45 mg NEP1–40-loaded microspheres, and 15 mg ChABC-loaded microtubes per scaffold., The ATIII bi-domain peptide (GNQEQVSPKβAFAKLAARLYRKA), synthesized by solid phase Fmoc chemistry as

previously described, was used to provide sustained growth factor delivery (GFs) [56, 57]. For scaffolds containing growth factors heparin, ATIII peptide, and growth factors were added to each fibrin scaffold. For scaffolds containing GFs and pMNs, the microspheres and microtubes were excluded from the formation solution. For scaffolds containing AIMS and pMNs, heparin, ATIII peptide, and growth factors were excluded from the formation solution. For scaffolds not containing cells, the pMNs were excluded from the formation solution (Table 1).

For implantation, a 10 μL fibrin scaffold was polymerized for 5 min then implanted into the created cavity. For groups containing pMNs, 10 EBs were added to the 10 μL scaffold during polymerization. A second 10 μL fibrin scaffold containing only $CaCl_2$ and thrombin was polymerized *in situ* to secure the initial scaffold within the lesion cavity. Following implantation, the spinal cord was covered with artificial dura, the back muscle closed with sutures, and the skin stapled closed. Upon completion of the surgery, animals were given buprenorphine and cefazolin in the same doses as specified for the initial injury. Bladders were manually expressed twice a day until normal bladder function returned. To limit immune rejection of the mouse cells, daily injections of cyclosporine-A (10 mg/kg, Novartis) were given. Two weeks after scaffold implantation, animals were euthanized by an overdose of Euthasol, and a transcardial perfusion performed with 4% paraformaldehyde. Spinal cords were harvested and post-fixed in 4% paraformaldehyde for 24 hours. After fixing, cords were cryoprotected in 30% sucrose in 10 mM PBS. Cords were embedded in Tissue-Tek OCT compound, frozen, and cut into 20 μm sagittal sections with a cryostat (Leica CM1950).

Immunohistochemistry

To determine expression of markers at the site of injury, immunohistochemistry was performed on 6 spinal cord sections per animal. OCT was washed from spinal cord sections with PBS. Sections were permeabilized with 0.1% Triton X-100 for 15 minutes and blocked with 10% bovine serum albumin and 2% normal goat serum (NGS). The following primary antibodies were applied overnight at 4°C in PBS with 2% NGS: β-tubulin III (β-tubIII, Covance, Dedham, MA, 1:400), glial fibrillary acidic protein (GFAP, ImmunoStar, 1:100), chondroitin sulfate (CS56, Sigma, 1:250), CD68 (ED1, AbD Serotec, 1:200), neuronal nuclei (NeuN, EMD Millipore, 1:500). Primary antibody staining was followed by 3 washes with PBS. Appropriate Alexa Fluor secondary antibodies (Life Technologies) in PBS with 2% NGS were applied for 2 hours at room temperature followed by an additional 3 washes in PBS. Sections were mounted using ProLong Gold anti-fade reagent with DAPI (Life Technologies).

Image Analysis of Immunohistochemistry

To quantify the staining of markers at the injury site, a series of images spanning the spinal cord were captured using an Optronics MICROfire camera (Optronics, Muskogee, OK) attached to an Olympus IX70 (Olympus, Center Valley, PA) inverted microscope with a 4× objective. As previously described, the images were merged using Adobe Photoshop, and the lesion site traced and expanded 250 μm away from the injury [14]. The lesion site was determined by staining for GFAP and tracing the border, the GFAP border between the host

tissue and lesion area was used to visualize the border for other stains. The average pixel intensity within the lesion area or 250 μm from the lesion border was measured using a custom Matlab (Mathworks, Natick, MA) script that determined the intensity of each individual pixel and then averaged all the intensities of pixels within the defined area. To compare the pixel intensity of stains between groups, all sections were stained and imaged at the same time. The exposure time and gain were not changed during imaging for individual stains and the sections were protected from light to limit photobleaching of the fluorophores.

Statistical Analysis

In vitro data was analyzed by ANOVA followed by Scheffe's post-hoc test with a significance criterion of 95%. Statistical significance for *in vivo* studies was determined by using the non-parametric Kruskal-Wallis one-way analysis of variance with a significance criterion of 95%.

Results

pMN Survival is not Effected by Combination Therapy with AIMS *In Vitro*

To study the effect of AIMS on the viability of pMNs in long-term culture, puromycin-selected pMNs were cultured in 3D fibrin scaffolds containing either one or both AIMS for two weeks post-induction. A cell viability assay with flow cytometery was used to quantify cell survival (Figure 1). Fibrin scaffolds alone contained 93.4% live cells and 6.6% dead cells, while the inclusion of AIMS resulted in 90.1% live cells and 9.9% dead cells. No statistical differences were measured between the groups. Separating out the two AIMS resulted in 85.1% live cells and 14.9% dead cells when only ChABC-loaded lipid microtubes were included in fibrin scaffolds, and 89.1% live cells and 10.9% dead cells when only NEP1–40-loaded PLGA microspheres were included in fibrin scaffolds. Therefore, the AIMS do not affect survival of pMNs after two weeks in culture *in vitro*.

Fibrin Scaffolds with AIMS Decrease pMN Survival in a Sub-acute SCI Model

Following *in vitro* analysis, fibrin scaffolds containing pMNs, AIMS and the GF delivery system were transplanted into a sub-acute rat thoracic SCI model. Transplantation of the biomaterial scaffolds was delayed until two weeks after injury to allow stabilization of the lesion site and to improve transplanted cell survival. Five different groups were used to evaluate the effects of using combination therapies for SCI: (1) fibrin scaffolds with the heparin-based delivery of growth factors (GFs, n = 5), (2) fibrin scaffolds incorporating GFs with pMNs (GFs+pMNs, n=5), (3) fibrin scaffolds incorporating AIMS (AIMS, n=6), (4) fibrin scaffolds incorporating AIMS with pMNs (AIMS+pMNs, n=7), and (5) fibrin scaffolds incorporating GFs, AIMS, and pMNs (GFs+AIMS+pMNs, n=6). The transplanted pMNs ubiquitously express GFP under the β-actin promoter to allow visualization of cells.

Fluorescence imaging at two weeks post-transplantation confirmed survival of GFP^+ cells in all groups that contained pMNs within the fibrin scaffolds (Figure 2A–C). However, the total GFP^+ area within the spinal cords was significantly different between groups with and without AIMS (Figure 2D). The GFP^+ area was decreased 10-fold when AIMS were included, suggesting AIMS have a negative effect on cell viability *in vivo*. While examining

infiltration of inflammatory cells into and around the lesion site, large numbers of ED1$^+$ macrophages/microglia was observed when both pMNs and AIMS were included in the scaffolds. The lowest level of ED1 staining was seen in the AIMS alone and the GFs alone groups (Figure 3). Together these data suggest that the combination of AIMS and pMNs may lead to decreased transplanted cell survival due to an increased inflammatory response.

Neural Differentiation and Integration of Transplanted pMNs following SCI

Differentiation and axon extension of the surviving transplanted pMNs into mature neural cell fates was examined to determine if the transplanted cells were capable of becoming the appropriate cell types. Astrocytes and neurons were seen within GFP$^+$ areas. Astrocytes were visualized by staining for GFAP, with the strongest GFAP expression found at the border of the lesion and at the edges of the cell transplants (data not shown). No significant difference in GFAP expression was found between any groups, suggesting similar degrees of reactive gliosis. GFP$^+$ areas also stained strongly for neuronal nuclei (Figure 4). The pMNs+GFs group had significantly higher amounts of NeuN staining than other groups likely due to higher pMN survival. However, normalizing the number of NeuN$^+$ cells in GFP$^+$ areas by the GFP$^+$ area showed no difference in the density of neuronal nuclei (rough measure of the % of neurons from pMNs) between groups with transplanted cells was observed (Figure 4F). No NeuN$^+$ cells were seen within the injury area in groups not receiving transplanted pMNs. Staining for the oligodendrocyte marker, O4, was inconclusive (data not shown).

In groups that contained transplanted pMNs+GFs, staining for the neuronal cytoskeletal protein β-tubIII demonstrated robust axonal extension within the transplant area (Figure 5A). The pMNs+GFs group had the greatest level of axonal extension within the lesion area, significantly higher than all other groups (Figure 5B). The groups containing pMNs+AIMS (with or without GF) showed colocalization between β-tubIII and GFP expression, suggesting that the transplanted cells were capable of differentiating into neurons and extending axons. However, no differences in the total amount of β-tubIII were seen when compared to groups without pMNs, suggesting that although the pMNs differentiate into neurons the number of surviving cells was too low to have a significant impact on axonal extension. Axon density in the host tissue immediately surrounding the lesion was not significantly different between any groups.

In many cases where transplanted cells were adjacent to the lesion border, there were GFP$^+$ cell processes crossing the GFAP defined border and into host tissue (Figure 6). However only 2 out of 13 (15%) transplants containing pMNs+AIMS (with or without GFs) showed surviving pMNs adjacent to the host border and capable of extending processes into the host tissue. The lack of surviving cells limited the potential for bridging the host-graft interface compared to the pMNs+GFs group, which had robust GFP$^+$ extension into the host tissue in 4 out of 5 transplants (80%). These data suggest that although the inclusion of AIMS does not inhibit the differentiation of pMNs into neuronal cell fates *in vivo*, or inhibit the pMNs ability to bridge into the host tissue, the AIMS greatly limit the efficacy of the cell transplants by decreasing the number of surviving pMNs, which in turn decreases the possibility of transplanted cells functionally integrating with host neural tissue.

Combination Scaffolds Increase CSPG Deposition in and around the Injury Area compared to Fibrin Scaffolds with AIMS

Previous work in our lab and other lab's has shown that transplanting ChABC-loaded microtubes into the injured spinal cord reduces CSPG levels [48, 58]. The loaded ChABC remains active upon release from the microtubes and decreases CSPG deposition around the injury site in acute transplantation models. Transplantation of AIMS alone in the sub-acute injury did not significantly affect CS56 staining, which marks non-degraded CSPGs, compared to groups containing pMNs+GFs and GFs alone (Figure 7). However, the transplantation of pMNs+AIMS (with or without GFs) demonstrated a significant increase in CSPG deposition within the lesion site despite the delivery of ChABC. The trends seen within the injury area were maintained in the immediate host tissue (within 250 μm of the injury), but differences in CS56 staining were not apparent more than 250 μm beyond the lesion (Figure 7F). Thus it appears the combination of pMNs+AIMS or pMNs+GFs+AIMS leads to a significant increase in CSPGs, which may inhibit axonal extension and the formation of synaptic connections between transplanted cells and host tissue.

Discussion

The secondary injury following SCI results in significant cell loss and formation of a complex, highly inhibitory glial scar. Many therapeutic options have targeted single obstacles that limit recovery following injury, which typically result in modest functional improvements. Here we combined several potentially promising therapies into a fibrin-based tissue engineered scaffold to overcome multiple obstacles simultaneously, with the aim of enhancing recovery over single therapies. Specifically, we aimed to repopulate the cystic cavity and limit the inhibitory effects found within the glial scar. Transplanting pMNs with the sustained delivery of neurotrophic factors verified previous work showing transplanted cells survived and differentiated into the expected cell types [14]. REMOVED SENTENCE. Interestingly, the combination of AIMS with pMNs did not result in an additive effect of the single therapies. Incorporating both AIMS and pMNs into fibrin scaffolds, with or without GFs, decreased cell survival and failed to reduce CSPGs around the lesion site.

The *in vitro* analysis of pMNs with AIMS did not show any adverse effects on cell viability at two weeks, which suggests that the AIMS only have a negative effect on pMN cell viability when transplanted *in vivo*. It is possible the AIMS indirectly limit survival through interactions with the host environment; specifically, the AIMS may increase recruitment of inflammatory cells, such as macrophages, when combined with cell transplants. Inflammatory cells, including neutrophils and macrophages, generate oxygen free radical species and lysosomal enzymes that cause non-specific degradation of the surrounding cells and tissue [59, 60]. Scaffolds containing AIMS did not significantly increase macrophage infiltration compared to GFs alone. The lipid microtubes were not expected to affect pMN viability and were previously shown to have a limited effect on the inflammatory response *in vivo* [54]. The sugar trehalose, used for thermostabilization of ChABC within the lipid microtubes, has been shown to increase cellular resistance to oxidative stress by scavenging free radicals and could limit the cytotoxic effects within the lesion site thus improving cell survival [61]. In contrast to the lipid microtubes, hydrolysis of PLGA microspheres creates

degradation byproducts that are acidic, lower the pH of the local environment, and have been shown to significantly affect cell viability in long term cultures [62]. Furthermore, subcutaneous implantation of PLGA scaffolds into adult rats showed an enhanced inflammatory response compared to less acidic scaffolds [63]. PLGA microspheres may increase long-term inflammation, but the AIMS incorporated into fibrin scaffolds without pMNs did not trigger increased macrophage infiltration. It is likely that individually, AIMS and pMNs both affect infiltration and activation of inflammatory cells, but the inflammation is limited until the two therapies are combined.

After transplantation, P-Olig2-derived pMNs retain high GFP expression, which colocalized to astrocyte (GFAP) and neuronal markers (NeuN), though oligodendrocyte (O4) staining was inconclusive. Importantly, the average density of $NeuN^+$ cells per GFP^+ area was consistent across all groups containing pMNs. The neuronal markers appeared within GFP^+ areas in much higher quantities compared to astrocyte markers. GFAP has been shown to be highly upregulated within reactive astrocytes, but has lower levels of expression in more growth permissive astrocytes [64, 65]. Therefore, the quantity of astrocytes may be higher than the GFAP staining suggests, and the astrocytes within the transplant area may be more growth permissive and less reactive than the host astrocytes located at the injury border.

Furthermore, the transplanted neurons extended robust axonal projections within the transplant area, bridged the injury site, and extended processes into the adjacent host tissue, which could enable synaptic connections between host and transplanted cells and possibly lead to functional circuits. Transplanted pMNs that survive two weeks post-transplantation are capable of differentiating into the appropriate cell fates in the presence of AIMs, demonstrating the feasibility of the combined system; and AIMS-induced inhibition to differentiation did not pose a significant obstacle. However it was clear that the combination of pMNs+AIMS had an overall negative effect on the transplanted cell survival, which led to decreased axonal extension. It would be expected that the transplanted cells that differentiate into neurons would result in an increase in axonal markers within the transplant area. However the number of surviving cells was too low to elicit an increase in staining for axonal processes compared to groups without transplanted pMNs. Therefore the pMNs +AIMS groups may not promote significant axonal extension and did not integrate with host tissue.

Lastly, the combination of AIMS and pMNs within fibrin scaffolds appears to have also had a negative impact on the surrounding extracellular environment by increasing the amount of CSPGs present within and around the injury area. Active ChABC was expected to degrade CSPGs in the local tissue, but became either inactive or phagocytosed prior to diffusing beyond the transplant area. Possible explanations of limited ChABC activity are the transplanted cells may directly influence the ChABC activity or the increased macrophage/microglia presence within the injury site may have reduced the ChABC activity. The higher CSPG deposition may also be a result of increased reactive gliosis. PLGA degradation byproducts can decrease the local pH, which has been shown to direct astrocytes into a reactive state [66]. However, no differences in GFAP staining were measured between groups, which would indicate an increase in reactive astrocytes. It is important to note that the AIMS group did not have significant decreases in CS56 staining compared to the GFs

group or the pMNs+GFs group. It is possible the amount of active ChABC delivered was not large enough to elicit significant decreases in CSPGs. Furthermore it would be expected that increased presence of CSPGs in the pMNs+AIMS groups (with or without GFs) would lead to decreased axonal extension, however no differences in axonal density were measured between any groups within the host tissue. The two week time point used in this study may limit the ability to measure significant differences between groups. The negative effects, such as increased inflammation caused by the combination therapies may occur several days after implantation and the increased CSPG deposition may occur after some axonal extension has already occurred. Therefore the CSPG increases may have had inadequate time to elicit measurable effects on axonal extension within the host tissue. It is possible that increased CSPGs would provide an inhibitory signal to axonal extension, resulting in decreased neural fiber staining at a later time point even though no differences in axonal extension were measured in this study.

Conclusion

Our lab has previously developed several therapeutic options that allow for cell transplantation of highly purified pMNs, the sustained delivery of neurotrophic factors, or the sustained delivery of ChABC and NEP1–40. In this study, we combined the therapeutic strategies within fibrin scaffolds with the aim of improving recovery over individual treatments. All treatments containing pMNs had viable cells two weeks post-transplantation into the injured spinal cord, although the incorporation of AIMS with pMNS led to a decrease in cell survival, possibly due to an enhanced inflammatory response within the lesion site. Surviving cells were capable of differentiating into neural cell fates and extending axons. Treatment options with AIMS in fibrin scaffolds showed a decreased presence of CSPGs, but this decrease was lost when AIMS and pMNs were combined. Future work will be improving the AIMS by decreasing their effect on pMN survival and limiting their effect on the inflammatory response. Studying the long-term effects of the combination therapies on functional recovery is important to understanding the how the transplants are incorporating into the host tissue.

Acknowledgements

This research was supported by the NIH R01 NS051454 and R01 NS090617 (SSE) and the NSF Graduate Research Fellowship (NSF DGE-1143954). Training in surgical technique and care was provided by OSU-SCITP, previously supported by the NIH/NINDS. Technical assistance was provided by Sara Oswald.

Disclosure:

SSE is an inventor on patents covering the heparin-binding delivery systems used for growth factor delivery in this study and may receive royalties from these patents. These patents are licensed by Kuros Therapeutics. No funding for this study was provided by Kuros.

REFERENCES

1. Chu TC, Zhoul HX, Li FY, Wang TY, Lu L, Feng SQ. Astrocyte transplantation for spinal cord injury: Current status and perspective. Brain Res Bull. 2014; 107:18–30. [PubMed: 24878447]
2. Ruff CA, Wilcox JT, Fehlings MG. Cell-based transplantation strategies to promote plasticity following spinal cord injury. Exp Neurol. 2012; 235:78–90. [PubMed: 21333647]

3. Davies SJA, Shih CH, Noble M, Mayer-Proschel M, Davies JE, Proschel C. Transplantation of Specific Human Astrocytes Promotes Functional Recovery after Spinal Cord Injury. Plos One. 2011; 6
4. Tetzlaff W, Okon EB, Karimi-Abdolrezaee S, Hill CE, Sparling JS, Plemel JR, et al. A systematic review of cellular transplantation therapies for spinal cord injury. Journal of neurotrauma. 2011; 28:1611–1682. [PubMed: 20146557]
5. Wu B, Sun L, Li PJ, Tian M, Luo YZ, Ren XJ. Transplantation of oligodendrocyte precursor cells improves myelination and promotes functional recovery after spinal cord injury. Injury. 2012; 43:794–801. [PubMed: 22018607]
6. Cao QL, Howard RM, Dennison JB, Whittemore SR. Differentiation of engrafted neuronal-restricted precursor cells is inhibited in the traumatically injured spinal cord. Exp Neurol. 2002; 177:349–359. [PubMed: 12429182]
7. Karimi-Abdolrezaee S, Eftekharpour E, Wang J, Morshead CM, Fehlings MG. Delayed transplantation of adult neural precursor cells promotes remyelination and functional neurological recovery after spinal cord injury. J Neurosci. 2006; 26:3377–3389. [PubMed: 16571744]
8. Mitsui T, Shumsky JS, Lepore AC, Murray M, Fischer I. Transplantation of neuronal and glial restricted precursors into contused spinal cord improves bladder and motor functions, decreases thermal hypersensitivity, and modifies intraspinal circuitry. J Neurosci. 2005; 25:9624–9636. [PubMed: 16237167]
9. Neuhuber B, Barshinger AL, Paul C, Shumsky JS, Mitsui T, Fischer I. Stem cell delivery by lumbar puncture as a therapeutic alternative to direct injection into injured spinal cord. J Neurosurg-Spine. 2008; 9:390–399. [PubMed: 18939929]
10. Parr AM, Kulbatski I, Zahir T, Wang X, Yue C, Keating A, et al. Transplanted adult spinal cord-derived neural stem/progenitor cells promote early functional recovery after rat spinal cord injury. Neuroscience. 2008; 155:760–770. [PubMed: 18588947]
11. Johnson PJ, Tatara A, McCreedy DA, Shiu A, Sakiyama-Elbert SE. Tissue-engineered fibrin scaffolds containing neural progenitors enhance functional recovery in a subacute model of SCI. Soft Matter. 2010; 6:5127–5137. [PubMed: 21072248]
12. Erceg S, Ronaghi M, Stojkovic M. Human Embryonic Stem Cell Differentiation Toward Regional Specific Neural Precursors. Stem Cells. 2009; 27:78–87. [PubMed: 18845761]
13. Rossi SL, Nistor G, Wyatt T, Yin HZ, Poole AJ, Weiss JH, et al. Histological and functional benefit following transplantation of motor neuron progenitors to the injured rat spinal cord. Plos One. 2010; 5:e11852. [PubMed: 20686613]
14. McCreedy DA, Wilems TS, Xu H, Butts JC, Brown CR, Smith AW, et al. Survival, differentiation, and migration of high-purity mouse embryonic stem cell-derived progenitor motor neurons in fibrin scaffolds after sub-acute spinal cord injury. Biomater Sci-Uk. 2014; 2:1672–1682.
15. Schnell L, Schneider R, Kolbeck R, Barde YA, Schwab ME. Neurotrophin-3 Enhances Sprouting of Corticospinal Tract during Development and after Adult Spinal-Cord Lesion. Nature. 1994; 367:170–173. [PubMed: 8114912]
16. Grill R, Murai K, Blesch A, Gage FH, Tuszynski MH. Cellular delivery of neurotrophin-3 promotes corticospinal axonal growth and partial functional recovery after spinal cord injury. J Neurosci. 1997; 17:5560–5572. [PubMed: 9204937]
17. Grill RJ, Blesch A, Tuszynski MH. Robust growth of chronically injured spinal cord axons induced by grafts of genetically modified NGF-secreting cells. Exp Neurol. 1997; 148:444–452. [PubMed: 9417824]
18. Ye JH, Houle JD. Treatment of the chronically injured spinal cord with neurotrophic factors can promote axonal regeneration from supraspinal neurons. Exp Neurol. 1997; 143:70–81. [PubMed: 9000447]
19. Jakeman LB, Wei P, Guan Z, Stokes BT. Brain-derived neurotrophic factor stimulates hindlimb stepping and sprouting of cholinergic fibers after spinal cord injury. Exp Neurol. 1998; 154:170–184. [PubMed: 9875278]
20. Menei P, Montero-Menei C, Whittemore SR, Bunge RP, Bunge MB. Schwann cells genetically modified to secrete human BDNF promote enhanced axonal regrowth across transected adult rat spinal cord. The European journal of neuroscience. 1998; 10:607–621. [PubMed: 9749723]

21. Liu Y, Kim D, Himes BT, Chow SY, Schallert T, Murray M, et al. Transplants of fibroblasts genetically modified to express BDNF promote regeneration of adult rat rubrospinal axons and recovery of forelimb function. J Neurosci. 1999; 19:4370–4387. [PubMed: 10341240]
22. Storer PD, Dolbeare D, Houle JD. Treatment of chronically injured spinal cord with neurotrophic factors stimulates betaII-tubulin and GAP-43 expression in rubrospinal tract neurons. Journal of neuroscience research. 2003; 74:502–511. [PubMed: 14598294]
23. Taylor L, Jones L, Tuszynski MH, Blesch A. Neurotrophin-3 gradients established by lentiviral gene delivery promote short-distance axonal bridging beyond cellular grafts in the injured spinal cord. J Neurosci. 2006; 26:9713–9721. [PubMed: 16988042]
24. Raff MC, Miller RH, Noble M. A Glial Progenitor-Cell That Develops Invitro into an Astrocyte or an Oligodendrocyte Depending on Culture-Medium. Nature. 1983; 303:390–396. [PubMed: 6304520]
25. Hart IK, Richardson WD, Bolsover SR, Raff MC. Pdgf and Intracellular Signaling in the Timing of Oligodendrocyte Differentiation. J Cell Biol. 1989; 109:3411–3417. [PubMed: 2557355]
26. Almad A, Sahinkaya FR, McTigue DM. Oligodendrocyte Fate after Spinal Cord Injury. Neurotherapeutics. 2011; 8:262–273. [PubMed: 21404073]
27. Kwok JCF, Warren P, Fawcett JW. Chondroitin sulfate: A key molecule in the brain matrix. Int J Biochem Cell B. 2012; 44:582–586.
28. McGee AW, Strittmatter SM. The Nogo-66 receptor: focusing myelin inhibition of axon regeneration. Trends Neurosci. 2003; 26:193–198. [PubMed: 12689770]
29. Kwok JCF, Dick G, Wang DF, Fawcett JW. Extracellular Matrix and Perineuronal Nets in CNS Repair. Dev Neurobiol. 2011; 71:1073–1089. [PubMed: 21898855]
30. Dickendesher TL, Baldwin KT, Mironova YA, Koriyama Y, Raiker SJ, Askew KL, et al. NgR1 and NgR3 are receptors for chondroitin sulfate proteoglycans. Nat Neurosci. 2012; 15:703–712. [PubMed: 22406547]
31. Fisher D, Xing B, Dill J, Li H, Hoang HH, Zhao ZZ, et al. Leukocyte Common Antigen-Related Phosphatase Is a Functional Receptor for Chondroitin Sulfate Proteoglycan Axon Growth Inhibitors. J Neurosci. 2011; 31:14051–14066. [PubMed: 21976490]
32. Shen YJ, Tenney AP, Busch SA, Horn KP, Cuascut FX, Liu K, et al. PTP sigma Is a Receptor for Chondroitin Sulfate Proteoglycan, an Inhibitor of Neural Regeneration. Science. 2009; 326:592–596. [PubMed: 19833921]
33. Bradbury EJ, Moon LDF, Popat RJ, King VR, Bennett GS, Patel PN, et al. Chondroitinase ABC promotes functional recovery after spinal cord injury. Nature. 2002; 416:636–640. [PubMed: 11948352]
34. Garcia-Alias G, Barkhuysen S, Buckle M, Fawcett JW. Chondroitinase ABC treatment opens a window of opportunity for task-specific rehabilitation. Nat Neurosci. 2009; 12 1145-U16.
35. Garcia-Alias G, Lin R, Akrimi SF, Story D, Bradbury EJ, Fawcett JW. Therapeutic time window for the application of chondroitinase ABC after spinal cord injury. Exp Neurol. 2008; 210:331–338. [PubMed: 18158149]
36. Moon LDF, Asher RA, Rhodes KE, Fawcett JW. Regeneration of CNS axons back to their target following treatment of adult rat brain with chondroitinase ABC. Nat Neurosci. 2001; 4:465–466. [PubMed: 11319553]
37. Wang DF, Ichiyama RM, Zhao RR, Andrews MR, Fawcett JW. Chondroitinase Combined with Rehabilitation Promotes Recovery of Forelimb Function in Rats with Chronic Spinal Cord Injury. J Neurosci. 2011; 31:9332–9344. [PubMed: 21697383]
38. Zuo J, Neubauer D, Dyess K, Ferguson TA, Muir D. Degradation of chondroitin sulfate proteoglycan enhances the neurite-promoting potential of spinal cord tissue. Exp Neurol. 1998; 154:654–662. [PubMed: 9878200]
39. Wang XX, Chun SJ, Treloar H, Vartanian T, Greer CA, Strittmatter SM. Localization of Nogo-A and Nogo-66 receptor proteins at sites of axon-myelin and synaptic contact. J Neurosci. 2002; 22:5505–5515. [PubMed: 12097502]
40. Schnaar RL. Brain gangliosides in axon-myelin stability and axon regeneration. Febs Lett. 2010; 584:1741–1747. [PubMed: 19822144]

41. Lee JK, Zheng B. Role of myelin-associated inhibitors in axonal repair after spinal cord injury. Exp Neurol. 2012; 235:33–42. [PubMed: 21596039]
42. Fournier AE, GrandPre T, Strittmatter SM. Identification of a receptor mediating Nogo-66 inhibition of axonal regeneration. Nature. 2001; 409:341–346. [PubMed: 11201742]
43. Domeniconi M, Cao Z, Spencer T, Sivasankaran R, Wang K, Nikulina E, et al. Myelin-associated glycoprotein interacts with the Nogo66 receptor to inhibit neurite outgrowth. Neuron. 2002; 35:283–290. [PubMed: 12160746]
44. Liu BP, Fournier A, GrandPre T, Strittmatter SM. Myelin-associated glycoprotein as a functional ligand for the Nogo-66 receptor. Science. 2002; 297:1190–1193. [PubMed: 12089450]
45. Wang KC, Koprivica V, Kim JA, Sivasankaran R, Guo Y, Neve RL, et al. Oligodendrocyte-myelin glycoprotein is a Nogo receptor ligand that inhibits neurite outgrowth. Nature. 2002; 417:941–944. [PubMed: 12068310]
46. GrandPre T, Li SX, Strittmatter SM. Nogo-66 receptor antagonist peptide promotes axonal regeneration. Nature. 2002; 417:547–551. [PubMed: 12037567]
47. Jones LL, Tuszynski MH. Chronic intrathecal infusions after spinal cord injury cause scarring and compression. Microsc Res Techniq. 2001; 54:317–324.
48. Wilems TS, Sakiyama-Elbert SE. Sustained dual drug delivery of anti-inhibitory molecules for treatment of spinal cord injury. J Control Release. 2015; 213:103–111. [PubMed: 26122130]
49. McCreedy DA, Rieger CR, Gottlieb DI, Sakiyama-Elbert SE. Transgenic enrichment of mouse embryonic stem cell-derived progenitor motor neurons. Stem Cell Res. 2012; 8:368–378. [PubMed: 22297157]
50. Quitschke WW, Lin ZY, Depontizilli L, Paterson BM. The Beta-Actin Promoter - High-Levels of Transcription Depend Upon a Ccaat Binding-Factor. J Biol Chem. 1989; 264:9539–9546. [PubMed: 2722849]
51. Seiler-Tuyns A, Eldridge JD, Paterson BM. Expression and regulation of chicken actin genes introduced into mouse myogenic and nonmyogenic cells. Proceedings of the National Academy of Sciences of the United States of America. 1984; 81:2980–2984. [PubMed: 6328484]
52. Willerth SM, Faxel TE, Gottlieb DI, Sakiyama-Elbert SE. The effects of soluble growth factors on embryonic stem cell differentiation inside of fibrin scaffolds. Stem Cells. 2007; 25:2235–2244. [PubMed: 17585170]
53. Kim H, Tator CH, Shoichet MS. Design of protein-releasing chitosan channels. Biotechnol Progr. 2008; 24:932–937.
54. Meilander NJ, Yu XJ, Ziats NP, Bellamkonda RV. Lipid-based microtubular drug delivery vehicles. J Control Release. 2001; 71:141–152. [PubMed: 11245915]
55. Willerth SM, Arendas KJ, Gottlieb DI, Sakiyama-Elbert SE. Optimization of fibrin scaffolds for differentiation of murine embryonic stem cells into neural lineage cells. Biomaterials. 2006; 27:5990–6003. [PubMed: 16919326]
56. Sakiyama-Elbert SE, Hubbell JA. Controlled release of nerve growth factor from a heparin-containing fibrin-based cell ingrowth matrix. J Control Release. 2000; 69:149–158. [PubMed: 11018553]
57. Sakiyama-Elbert SE, Hubbell JA. Development of fibrin derivatives for controlled release of heparin-binding growth factors. J Control Release. 2000; 65:389–402. [PubMed: 10699297]
58. Lee H, McKeon RJ, Bellamkonda RV. Sustained delivery of thermostabilized chABC enhances axonal sprouting and functional recovery after spinal cord injury. Proceedings of the National Academy of Sciences of the United States of America. 2010; 107:3340–3345. [PubMed: 19884507]
59. Cassatella MA. The production of cytokines by polymorphonuclear neutrophils. Immunology today. 1995; 16:21–26. [PubMed: 7880385]
60. Taoka Y, Okajima K. Role of leukocytes in spinal cord injury in rats. Journal of neurotrauma. 2000; 17:219–229. [PubMed: 10757327]
61. Benaroudj N, Lee DH, Goldberg AL. Trehalose accumulation during cellular stress protects cells and cellular proteins from damage by oxygen radicals. J Biol Chem. 2001; 276:24261–24267. [PubMed: 11301331]

62. Sung HJ, Meredith C, Johnson C, Galis ZS. The effect of scaffold degradation rate on three-dimensional cell growth and angiogenesis. Biomaterials. 2004; 25:5735–5742. [PubMed: 15147819]

63. Kim MS, Ahn HH, Shin YN, Cho MH, Khang G, Lee HB. An in vivo study of the host tissue response to subcutaneous implantation of PLGA- and/or porcine small intestinal submucosa-based scaffolds. Biomaterials. 2007; 28:5137–5143. [PubMed: 17764737]

64. Bardehle S, Kruger M, Buggenthin F, Schwausch J, Ninkovic J, Clevers H, et al. Live imaging of astrocyte responses to acute injury reveals selective juxtavascular proliferation. Nat Neurosci. 2013; 16 580-+

65. Pekny M, Wilhelmsson U, Pekna M. The dual role of astrocyte activation and reactive gliosis. Neurosci Lett. 2014; 565:30–38. [PubMed: 24406153]

66. Oh TH, Markelonis GJ, Von Visger JR, Baik B, Shipley MT. Acidic pH rapidly increases immunoreactivity of glial fibrillary acidic protein in cultured astrocytes. Glia. 1995; 13:319–322. [PubMed: 7615340]

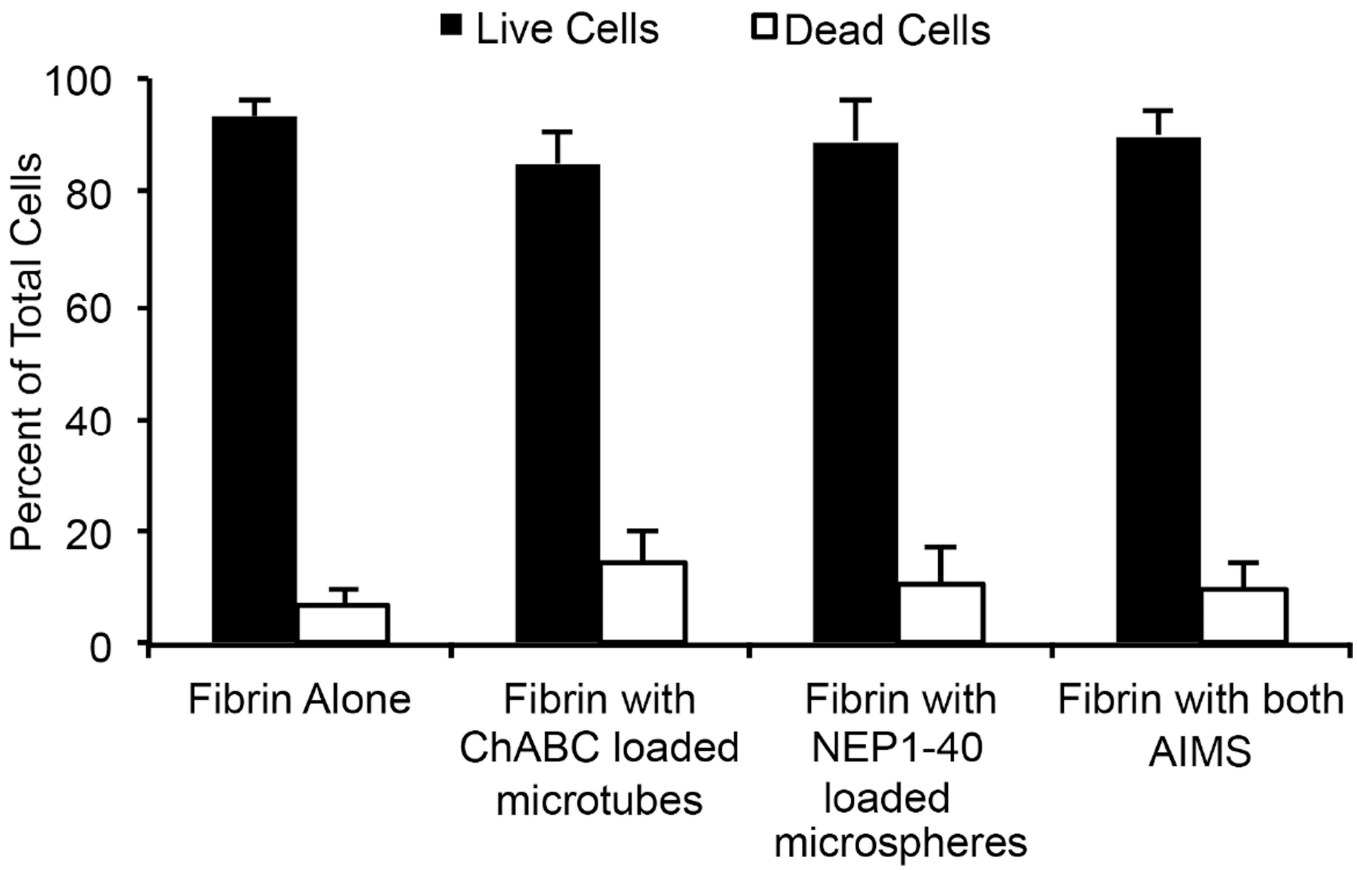

Figure 1. Viability of purified pMNs cultured in fibrin scaffolds with or without AIMS at two weeks *in vitro*

Flow cytometery quantification of the percentage of live and dead cells after degradation of scaffolds. Live cells stained positive with calcein AM and dead cells stained positive with ethidium homodimer-1. No significant differences were seen between groups. Error bars are standard deviation.

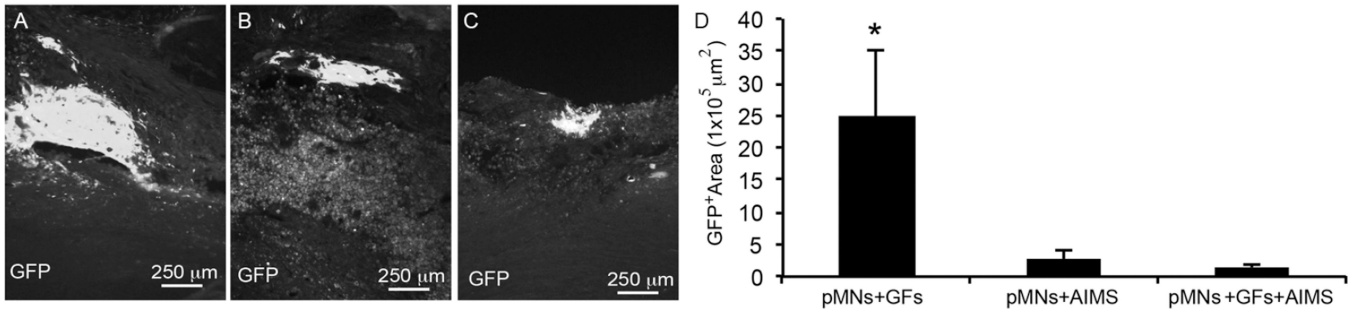

Figure 2. Effect of combination therapies on transplanted pMNs in injured spinal cord sections two weeks after transplantation

(A–C) Representative images of GFP^+ areas within the (A) pMNs+GFs group, (B) pMNs +AIMS group, and (C) pMNs+GFs+AIMS group. **(D)** The average GFP^+ area within the lesion site was determined. GFP expression was significantly decreased in groups containing AIMS and pMNs compared to the pMNs+GFs group. Error bars are standard deviation. * denotes significant difference versus other groups ($p<0.05$).

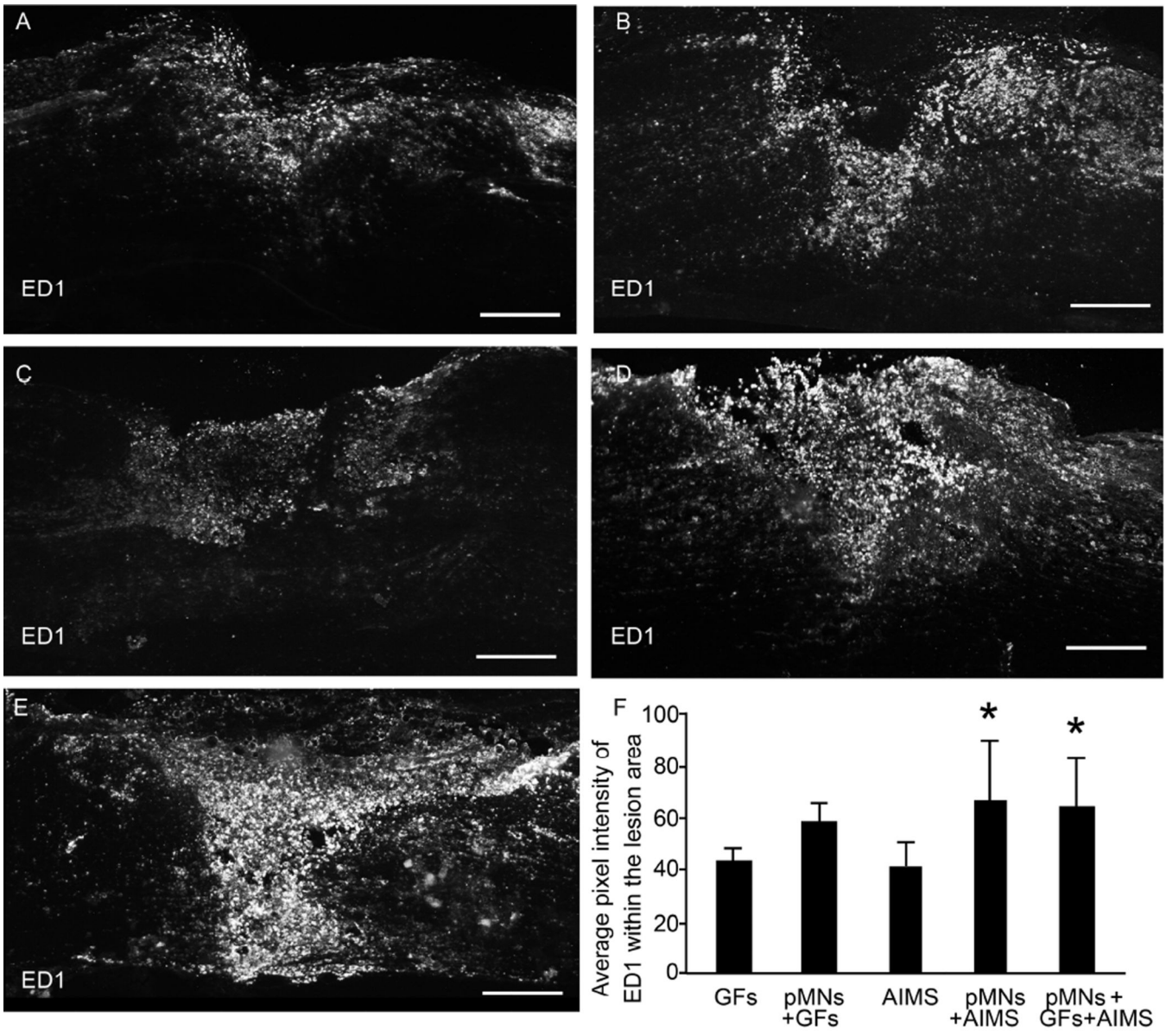

Figure 3. Effect of combining pMNs and AIMS on macrophage infiltration as assessed by ED1 staining

(A–E) Representative images of 20 μm thick sections of ED1 (marker for activated inflammatory cells) staining within and around the lesion site for groups containing (A) GFs, (B) pMNs+GFs, (C) AIMS, (D) pMNs+AIMS, (E) pMNs+GFs+AIMS. Positive staining for ED1 appears higher in groups containing both pMNs and AIMS. **(F)** The average pixel intensity of ED1 stained sections within the lesion area was determined. Fibrin scaffolds with pMNs+AIMS had significantly higher ED1 staining compared to AIMS. Error bars are standard deviation. * denotes $p<0.05$ versus the AIMS group. Scale bar is 250 μm.

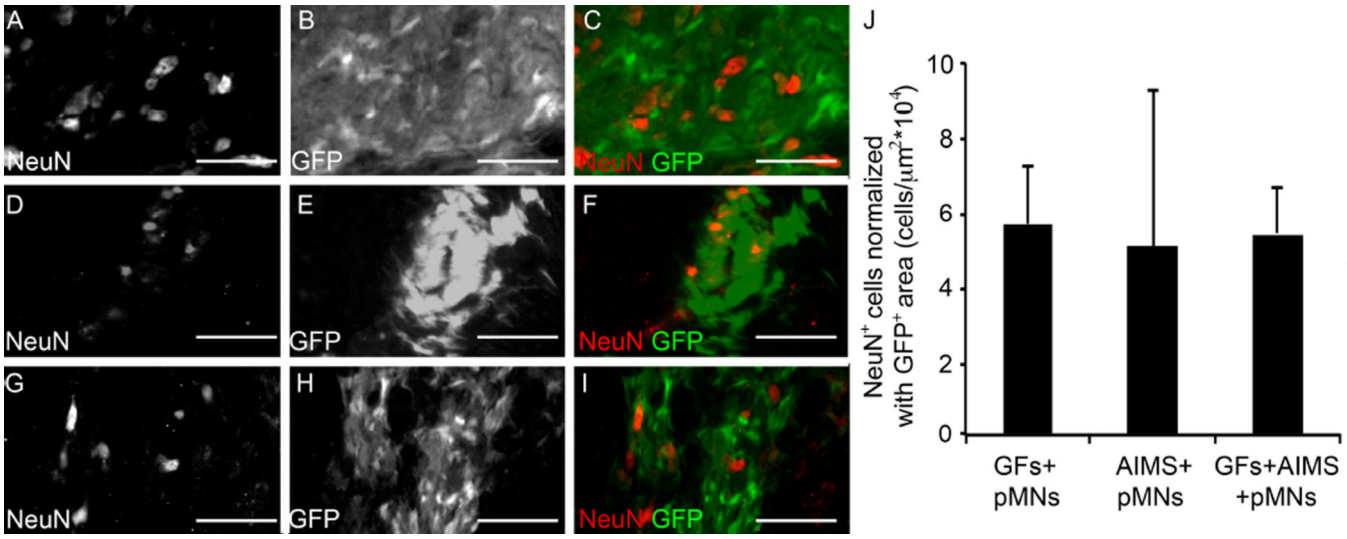

Figure 4. pMNs differentiate into neurons when transplanted into the injured spinal cord

(A–I) Representative images from GFs+pMNs, GFs+AIMS+pMNs, and AIMS+pMNs groups stained with the neuronal nuclei marker, NeuN, two weeks post-transplantation. **(A–C)** GFs+pMNs group showing $NeuN^+$ cells **(A)** and GFP^+ areas **(B)** that colocalize together **(C)**. **(D–F)** GFs+AIMS+pMNs groups also stained positive with NeuN **(D)** within GFP^+ areas **(E)** and showed colocalization **(F)**. **(G–I)** AIMS+pMNs also showed $NeuN^+$ cells **(G)** within GFP^+ areas **(H)** which colocalize together **(I)**. **(J)** The GFs+pMNs group had significantly greater GFP^+ area and higher numbers of $NeuN^+$ cells, but when $NeuN^+$ cell number is normalized by the GFP^+ area similar levels of NeuN expression between all groups. Scale bars are 100 μm. Error bars are standard deviation.

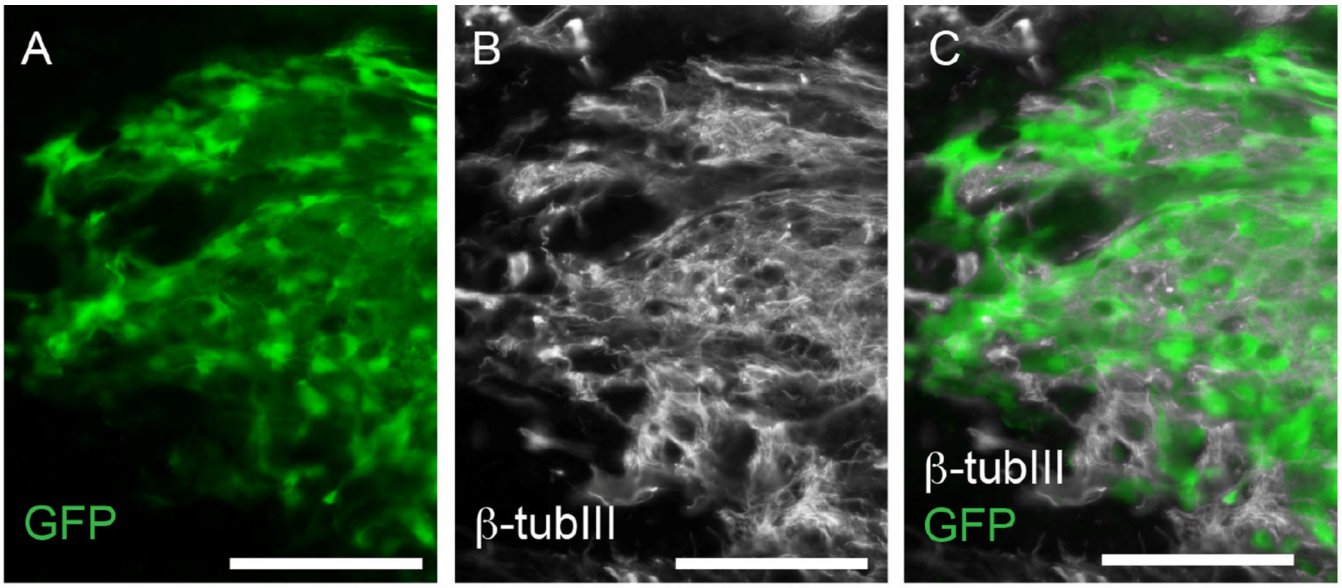

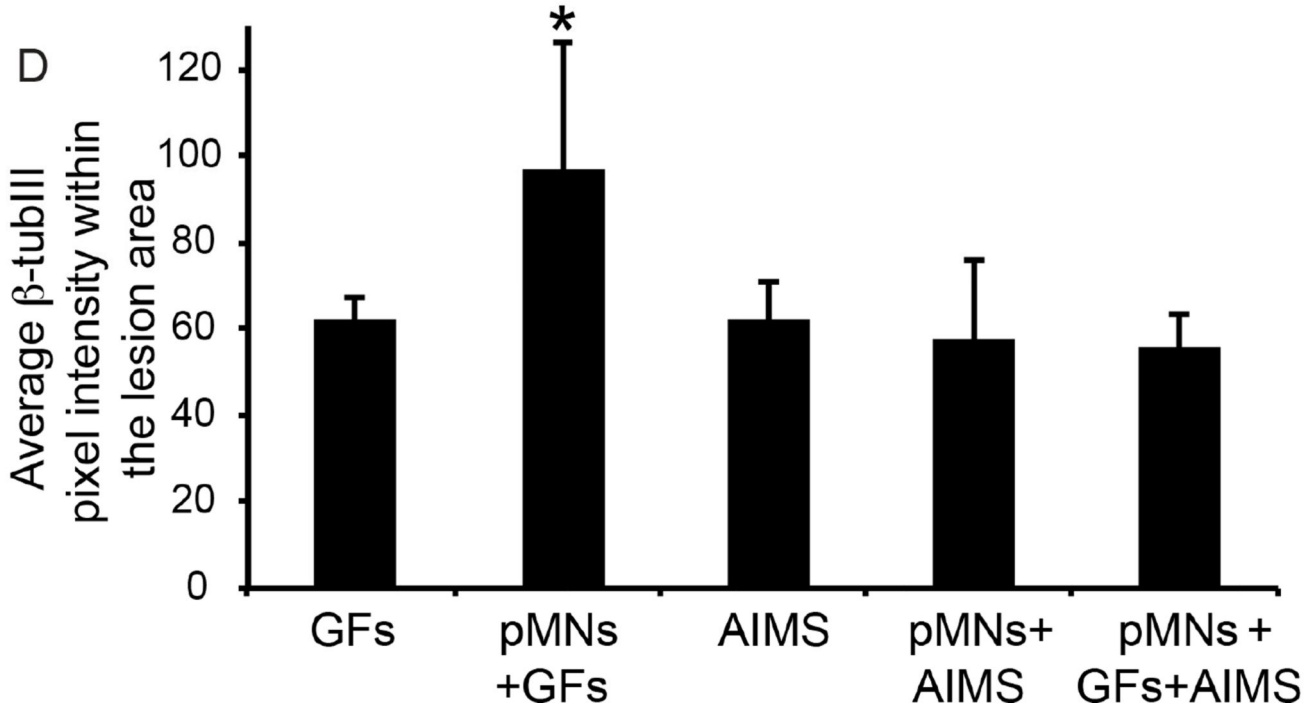

Figure 5. Spinal cord sections show colocalization of neuronal extensions and GFP$^+$ areas

(A–C) Representative images of GFP expression and a marker for neurons, β-tubIII, from GFs+pMNs group **(A)** and β-tubIII staining **(B)** that shows colocalization when merged together **(C)**. Robust β-tubIII staining was observed overlapping with GFP$^+$ areas. **(D)** The average pixel intensity of β-tubIII staining in sections within the lesion area was determined. Error bars are standard deviation. Scale bar is 100 μm. * denotes $p<0.05$ versus all other groups.

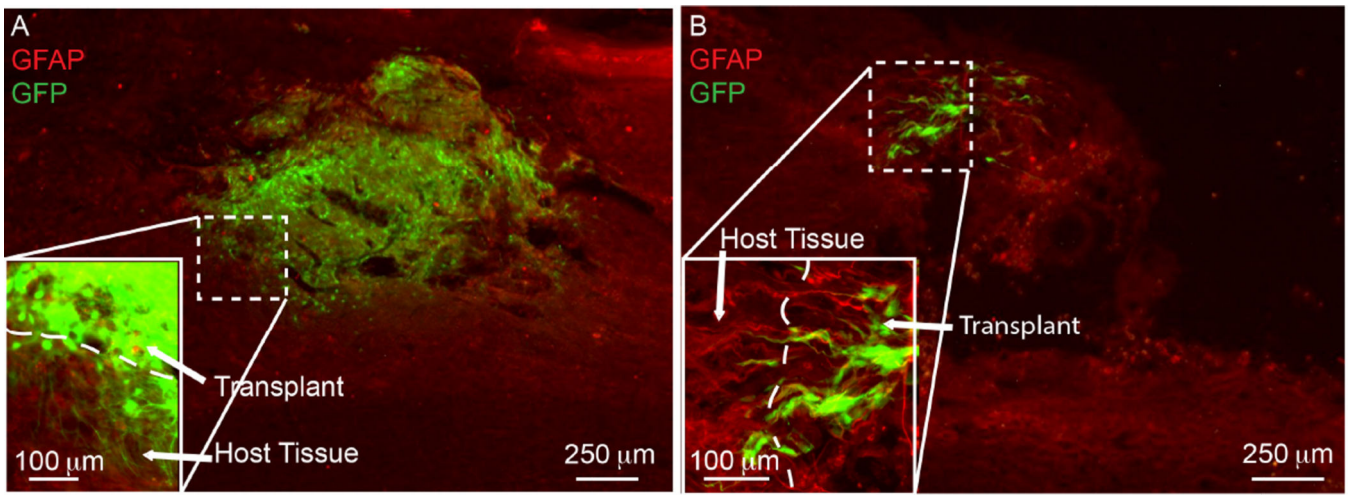

Figure 6. Penetration of transplanted pMNs into host tissue

Fluorescence images of injured spinal cord sections from **(A)** pMNs+GFs and **(B)** pMNs +GFs+AIMS were overlaid on top of the corresponding IHC images stained for the astrocyte specific marker (GFAP).

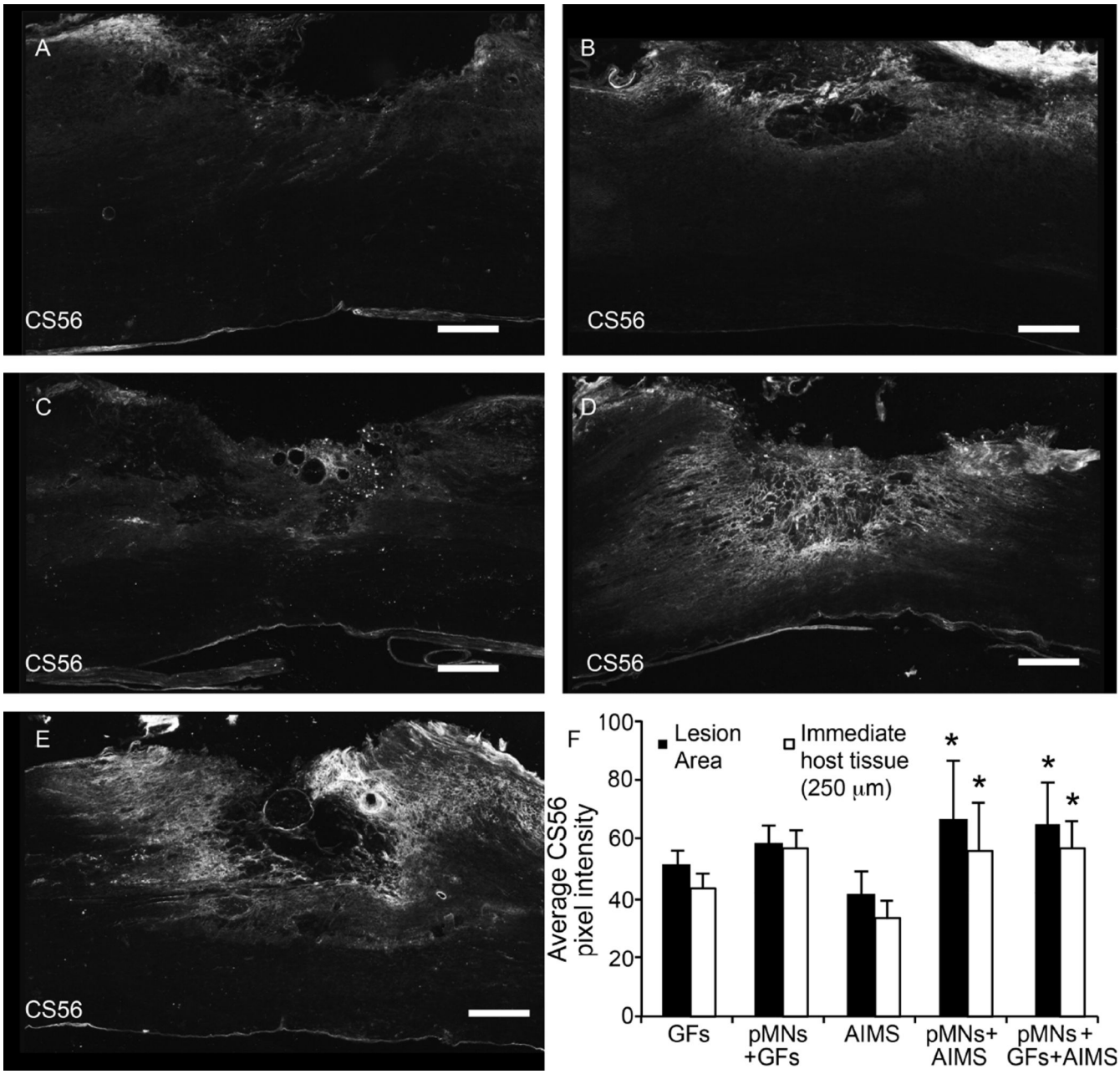

Figure 7. Combination of pMNs and/or GFs with AIMS does not decrease CSPGs compared to GFs alone or pMNs+GFs

(A–E) Representative images of CS56, a marker for non-degraded CSPGs, staining within and around the lesion site for groups containing (A) GFs, (B) pMNs+GFs, (C) AIMS, (D) pMNs+AIMS, (E) pMNs+GFs+AIMS. Strong CS56 staining was seen when pMNs and AIMS were included in fibrin scaffolds. **(F)** The average pixel intensity of CS56 stained sections within the lesion area and within the immediate host tissue (250 μm from the lesion border) was determined. Fibrin scaffolds with pMNs+AIMS or pMNs+GFs+AIMS had significantly higher CS56 staining compared to the AIMS alone group in both the lesion

area and immediate host tissue. Error bars are standard deviation. * denotes $p<0.05$ versus AIMS alone group.

Table 1

Design of SCI combination therapy study

All groups had fibrin as the scaffold and included some combination of heparin, ATIII peptide, GFs (NT-3 & PDGF), NEP1–40 PLGA microspheres, ChABC lipid microtubes, and pMNs.

Combination Scaffolds	Heparin	ATIII peptide	NT-3/PDGF	NEP1–40 PLGA microspheres	ChABC lipid microtubes	Selected pMNs
GFs (n=5)	X	X	X			
pMNs+GFs (n=5)	X	X	X			X
AIMS (n=6)				X	X	
pMNs+AIMS (n=7)				X	X	X
GFs+AIMS+pMNs (n=6)	X	X	X	X	X	X